Genetic diversity and demographic history of the largest remaining migratory population of blue wildebeest (*Connochaetes taurinus taurinus*) in southern Africa

Stephanie J. Szarmach[1,2], Katherine C. Teeter[1], Jassiel M'soka[3], Egil Dröge[4,5], Hellen Ndakala[6], Clive Chifunte[4,7], Matthew S. Becker[4,8], Alec R. Lindsay[1]

[1]Department of Biology, Northern Michigan University, Marquette, MI 49855, USA

[2]Department of Biology, Pennsylvania State University, State College, PA 16802, USA

[3]USAID Zambia, Lusaka, Zambia

[4]Zambian Carnivore Programme, Mfuwe, Eastern Province, Zambia

[5]Wildlife Conservation Research Unit, Department of Biology, The Recanati-Kaplan Centre, Oxford University, Oxford, United Kingdom

[6]Zambia Department of National Parks and Wildlife, Liuwa Plain

[7]Zambia Department of National Parks and Wildlife, Mumbwa, Zambia

[8]Department of Ecology, Montana State University, Bozeman, MT 59735, USA

Corresponding author: Stephanie J. Szarmach, stephszarmach@gmail.com

ORCID: 0000-0003-1538-8127

ACKNOWLEDGEMENTS

Our thanks to the Zambia Department of National Parks and Wildlife, African Parks Network, and the Barotse Royal Establishment for permission and collaboration in this research. We gratefully acknowledge the late Jeffrey Horn of the NMU Computer Science Department, who passed away in February 2024. Jeff provided the computing infrastructure and assistance that made the data analysis for this work possible. We appreciate and miss his enthusiasm for collaborating across disciplines. We also thank Grant Combs for computing assistance. We are very grateful to Michael Sorenson and Jeffrey DaCosta for guidance on the RAD-seq protocol and analysis pipeline. We also thank Kurt Galbreath for input and advice on the project and Catherine Sun for feedback on the manuscript.

ABSTRACT

The blue wildebeest (*Connochaetes taurinus taurinus*) is a keystone species in the savannahs of southern Africa, where it maintains shortgrass plains and serves as an important prey source for large carnivores. Despite being the second largest migratory wildebeest population, the wildebeest of the Greater Liuwa Ecosystem (GLE) of western Zambia have remained largely unstudied, until recently. While studies have increased understanding of recent demography, migration, and population limiting factors, the level of genetic diversity, patterns of gene flow, and long-term demographic history of blue wildebeest in the GLE remains unknown. Most genetic studies of wildebeest have focused on small, heavily-managed populations, rather than large, migratory populations of high conservation significance. We used restriction-site associated DNA sequencing (RAD-seq) to assess genetic diversity, population structure, and demographic history of blue wildebeest in the GLE. Using SNPs from 1,730 loci genotyped across 75 individuals, we found moderate levels of genetic diversity in GLE blue wildebeest (H_e = 0.210), no evidence of inbreeding (F_{IS} = 0.033), and an effective population size of about one tenth the estimated population size. No genetic population structure was evident within the GLE. Analyses of the site frequency spectrum found signatures of expansion during the Middle Pleistocene followed by population decline in the Late Pleistocene and early Holocene, a pattern previously observed in other African ungulates. These results will supplement field studies in developing effective conservation plans for wildebeest as they face continued and increasing threats of habitat loss, poaching, and other human impacts across their remaining range.

INTRODUCTION

The blue wildebeest (*Connochaetes taurinus*) is a large antelope that acts as a keystone species in the savannahs of southern and eastern Africa. Many wildebeest populations migrate seasonally in response to precipitation, availability of high-quality forage, and predation risk [1–4]. Grazing by wildebeest maintains shortgrass plains and facilitates nutrient cycling [5–7], which in turn supports communities of other grazing mammals, insects, and birds that depend on small herbaceous plants [8]. Carnivores, such as lions (*Panthera leo*), hyenas (*Crocuta crocuta*), wild dogs (*Lycaon pictus*), and cheetahs (*Acinonyx jubatus*), often depend on wildebeest as an important prey source [9–12]. Because of the significant ecological roles of wildebeest, changes in migration dynamics or population size could have dramatic impacts on other species and communities in the African grasslands [13].

In many parts of the wildebeest's range, habitat destruction and fragmentation, obstruction of migration routes, and poaching have impacted wildebeest population size and movement [14]. The conversion of grassland to agricultural fields has reduced available foraging area, contributing to population declines [15,16] and the construction of fences and roads has blocked migration routes and caused previously migratory populations to become sedentary [17,18]. Poaching for bushmeat, driven by deteriorating economic conditions in many communities in and around protected area networks, also threatens wildebeest populations [19–21]. To better understand and address the impact of these threats, there is a need to detect and evaluate their effects on populations.

In addition to experiencing recent declines, wildebeest populations may have undergone fluctuations in the more distant past due to changes in climate or human activity. Genetic analysis of other African ungulates, including African buffalo (*Syncerus caffer*) [22–24], African

elephant (*Loxodonta africana*) [25], and hippopotamus (*Hippopotamus amphibius*) [26,27], revealed population declines during the late Pleistocene and early Holocene. These declines coincide with increases in human population size and periods of aridity on the African continent, during which longer dry seasons led to drought and changes in water levels and vegetation types [28–30]. Because many wildebeest populations migrate in response to rainfall and vegetation growth and populations have declined during recent droughts, wildebeest likely experienced similar declines during these two epochs [4,19].

Large population declines during the Late Pleistocene and Holocene may have affected the level of genetic diversity found in the species today, and an understanding of these changes could help in evaluating future demographic effects of climate change. Today, the dryland ecosystems comprising most of the remaining wildebeest range are characterized by extreme seasonality in resource abundance and distribution, making mobility and access to these resources key, particularly in the face of climate change [31]. Understanding how continued habitat fragmentation, loss of migratory routes, and population declines affect genetic diversity and the ability of wildebeest to adapt to the rapidly changing environments of the Anthropocene is therefore of key importance.

The Greater Liuwa Ecosystem (GLE), located in western Zambia and encompassing Liuwa Plain National Park (3,660 km^2) and the Upper West Zambezi Game Management Area (22,156 km^2; Figure 1), supports a large, migratory blue wildebeest population. This flat, open grassland experiences extensive seasonal flooding, which drives the wildebeest to migrate between the drier, southern portion of the GLE, where they spend the wet season (November – April), and the previously flooded northern areas for the dry season (May – October) [32,33]. Though this is thought to be the second largest wildebeest migration in Africa, little was known

about this population until recently, after it experienced a significant decline. Poaching, driven by regional politics and civil war in neighboring Angola, led to severe declines of many species in the GLE, including wildebeest, and notably led to the extirpation of lions [32,34]. Additionally, while the wildebeest are thought to have historically migrated between Zambia and Angola, since the Angolan civil war (1975-2002) no transboundary migration has been observed and radio-tracking has shown wildebeest movements to be largely confined to the GLE [33].

Fig. 1. Location of study area. (a) Satellite map of Zambia and surrounding area with Liuwa Plain National Park, where blue wildebeest tissue samples were collected for this study, outlined in white and marked with a star. Basemap: Google Satellite (obtained through QuickMapServices QGIS plugin), Map data © 2024 Google. (b) Image of a blue wildebeest (Photograph by S. Szarmach). (c) Location of Zambia (green) within Africa.

Restoration efforts in Liuwa began in 2003 with the signing of a 20-year management agreement between the government of Zambia and African Parks Network. Ecosystem recovery efforts have resulted in growth and stabilization of the wildebeest population, from an estimated 15,000 individuals in 2001 to 46,000 in 2013 [33–35]. Studies of movement, demography, environmental influences, and predator-prey dynamics [11,32,33,36] have improved understanding of wildebeest population dynamics in the GLE, but the amount of genetic diversity present in the population and its long-term demographic history remain unknown. Past changes in population size have important implications for conservation in the present day, because historical bottlenecks can reduce genetic diversity and limit future adaptive potential, and the comparison of present day to past effective population sizes can improve understanding of current conservation risks for the population [37,38].

125 Despite the wildebeest being an iconic species of the African savannahs with high
126 conservation significance, until very recently [39], few genetic studies of wildebeest had been
127 published. Studies utilizing molecular markers can inform wildlife management by delineating
128 conservation units, revealing inbreeding, and divulging historical patterns of movement and
129 demographic change [40,41]. Most previous genetic studies of wildebeest focused on heavily
130 managed populations in South Africa, and few evaluated the potential impacts of habitat loss,
131 fragmentation, and population declines occurring across remaining wildebeest range. Early
132 studies assessing wildebeest genetic diversity used allozymes, microsatellites or mitochondrial
133 DNA primarily to inform management of small populations of wildebeest on game ranches in
134 South Africa [42–44]. Microsatellite and mtDNA studies that included samples from a greater
135 part of the blue wildebeest's range identified high levels of genetic divergence between
136 wildebeest in southern versus eastern Africa, as well as lower levels of significant differentiation
137 between pairs of populations within these regions [45,46].
138 More recently, whole-genome resequencing of blue wildebeest from much of the species'
139 range found significant genetic differentiation between all subspecies of blue wildebeest, as well
140 as between local populations of the western white bearded (*C. t. mearnsi*) subspecies in eastern
141 Africa and the brindled (*C. t. taurinus*) subspecies in southern Africa [39]. Importantly, Liu et al.
142 [39] found that wildebeest populations where migration had recently been disrupted showed
143 lower genetic diversity and higher levels of inbreeding compared to fully migratory populations.
144 No previous genetic studies have included wildebeest from the GLE, despite this being one of
145 the largest migratory wildebeest populations. The effects of past changes in population size, both
146 historical and recent, on genetic diversity in this recovering migratory population remain
147 unknown.

148 We assessed genetic diversity, population structure, and demographic history of the GLE
149 blue wildebeest population using a genome-wide SNP dataset generated through restriction-site
150 associated DNA sequencing (RAD-seq). We first evaluated the current level of genetic diversity
151 present in the GLE wildebeest population, estimated contemporary effective population size, and
152 assessed whether genetic population structure is present. We used both model-based
153 (STRUCTURE) and model-free (PCA) approaches to determine whether multiple populations
154 exhibiting significant differences in SNP allele frequencies are present within the GLE, or
155 whether this region is occupied by a single, panmictic population. We then inferred the past
156 demographic history of the GLE blue wildebeest population and tested the hypothesis that
157 genetic signatures of population contraction are present due to past climate change and
158 anthropogenic pressures. To do this, we tested demographic models using the coalescent
159 simulator fastsimcoal2 [47] and implemented the model-independent stairway plot method
160 [48,49] to estimate effective population size over time based on the site frequency spectrum.
161

162 **MATERIALS AND METHODS**

163 *Sample collection and DNA extraction*

164 As part of long-term field studies conducted with the Zambia Department of National Parks and
165 Wildlife (DNPW) and African Parks, we collected 97 tissue samples in the GLE between
166 2011−2014 from wildebeest that were anesthetized for radio collaring as part of long-term
167 studies, or from opportunistically sampled wildebeest carcasses detected during the course of
168 fieldwork. These tissue samples were transferred to ethanol for storage. All animal handling
169 procedures were performed following animal welfare standards and protocols required by the
170 Zambia Department of Veterinary and Livestock Services and the DNPW and were approved by

171 the Montana State University IACUC. Samples were exported with Zambia Wildlife Authority
172 Permit #7830 and imported with USDA Veterinary Permit #109174. We extracted genomic
173 DNA from the tissues using the DNeasy Blood & Tissue Kit (Qiagen, Valencia, CA, USA) and
174 quantified the concentration and purity of the extracted DNA using a Nanodrop 2000c. DNA
175 extractions with a concentration <10 ng/μL were combined with DNA from a second extraction
176 from the same tissue sample, if available, and concentrated using vacuum centrifugation.
177
178 *RAD library preparation and sequencing*
179 We prepared double-digest restriction site associated DNA (ddRAD) libraries following the
180 protocol of DaCosta and Sorenson [50]. First, ~1 μg of genomic DNA from each wildebeest was
181 digested using the restriction enzymes *EcoR*I-HF and *Sbf*I-HF (New England Biolabs, Ipswich,
182 MA, USA). Unique combinations of barcoded adapters were ligated to the digested DNA from
183 each individual, so that samples could later be pooled for sequencing. Restriction fragments
184 within a size range of 200−400 bp were selected through gel excision, and DNA was purified
185 using a Qiagen MinElute Gel Extraction Kit. The size-selected DNA fragments were PCR
186 amplified using Phusion High-Fidelity PCR Master Mix (Thermo Scientific, Waltham, MA,
187 USA). PCR products were purified with AMPure XP SPRI beads (Beckman Coulter, Brea, CA,
188 USA). The concentrations of the purified PCR products were quantified using real-time PCR,
189 and samples were pooled in equimolar amounts, with the exception of some low-concentration
190 samples. Ultimately, 83 samples were included in the multiplexed library, which was sequenced
191 on one lane of an Illumina HiSeq 2500 Sequencing System (Tufts University, Medford, MA,
192 USA), generating single-end reads of 100 bp in length.
193

194 *Alignment, genotyping, and quality filtering*

195 After sequencing, we used FastQC version 0.11.7 to assess per-base sequence quality for the
196 reads [51]. We used a computational pipeline developed by DaCosta and Sorenson [50] for
197 analyzing ddRAD-seq data to process the raw sequence reads (Python scripts available at
198 https://github.com/BU-RAD-seq/ddRAD-seq-Pipeline). After correcting sequencing errors in
199 restriction sites and barcodes, reads were assigned to individual wildebeest based on the
200 combination of barcodes associated with the read. The demultiplexed sequence data are available
201 from the NCBI Sequence Read Archive (SRA) under the following accession numbers:
202 BioProject ID PRJNA588629; BioSample IDs SAMN13254976−SAMN13255074. After
203 demultiplexing, identical sequences were collapsed and reads with low average Phred quality
204 scores (Q < 20) were filtered out. The condensed and filtered reads were then clustered into
205 putative loci across individuals based on a similarity threshold of 0.85 using the UCLUST
206 algorithm in the program USEARCH version 5 [52]. A representative sequence from each cluster
207 was aligned to a reference genome using the blastn program in BLAST version 2.8.0 [53] and the
208 following settings: evalue = 0.0001, word_size = 11, gapopen = 5, gapextend = 2, penalty = -3,
209 reward = 1, and dust = yes). Sequences were aligned to two reference genomes: version 4.0 of
210 the domestic sheep (*Ovis aries*) genome (2015; Assembly GCA_000298735.2), downloaded
211 from NCBI, and the blue wildebeest genome sequenced and assembled by Chen et al. [54],
212 downloaded from http://animal.nwsuaf.edu.cn/code/index.php/Ruminantia. Separate clusters that
213 generated BLAST hits to the same genomic location were combined into a single cluster, and
214 those that did not generate hits to the reference genome were retained but marked as anonymous
215 loci. Reads were aligned within each cluster using MUSCLE version 3.8.31 [55].

216 We genotyped individuals at the identified loci using DaCosta and Sorenson's
217 RADGenotypes.py script [50], which calls individuals as homozygous for a SNP if >93% of
218 reads exhibit the same allele, and as heterozygous if >29% of reads show a second allele. When a
219 lower proportion of reads exhibited a minor allele, the genotype was flagged as a "provisional
220 heterozygote" (20-29% of reads) or "ambiguous" (7-20%) and was required to pass additional
221 examination and quality filtering before being included in the final set of SNPs. A custom R
222 script utilizing the tidyverse collection of packages [56,57] was used to remove loci with
223 substantial amounts of missing data and putative "paralogous loci" formed by erroneous
224 clustering of sequences originating from repetitive elements in the genome (R script available at
225 https://github.com/sszarmach/NMU-wildebeest). Samples with an average sequencing depth of
226 <10 reads per locus and loci with <5 reads in >10% of samples were removed, since low
227 sequencing depth can lead to genotyping errors [58]. We filtered out loci that significantly
228 departed from Hardy-Weinberg equilibrium based on a chi-square goodness-of-fit test ($\alpha = 0.05$),
229 because such deviation can result from null alleles (heterozygote deficiency) or incorrectly
230 clustered paralogous loci (heterozygote excess). To eliminate putative paralogous loci, we also
231 removed clusters that exhibited more than two alleles, that had abnormally high read depths
232 (mean depth >700), that had >4 SNPs, or that generated multiple high-quality BLAST hits to the
233 reference genome [59,60]. For all downstream analyses except inference of demographic history
234 using the site frequency spectrum, a minor allele frequency filter (MAF >0.01) was applied to
235 remove loci containing singleton SNPs, which could be an artifact of sequencing error. These
236 quality filtering steps are outlined in Supplementary Table 1.
237
238 *Genetic diversity*

239 A final data set of 1,730 polymorphic loci genotyped across 75 individuals was used to calculate
240 summary statistics describing genetic diversity in GLE blue wildebeest. We randomly drew one
241 SNP from each RAD locus to avoid the inclusion of multiple SNPs that were linked due to
242 chromosomal proximity. We used PGDSpider version 2.1.1.5 to convert the SNP data file into
243 the correct format for each analysis program [61]. Allele frequencies and expected and observed
244 heterozygosities were calculated using the R package adegenet [62,63]. We tested SNPs for
245 deviation from Hardy-Weinberg equilibrium using the hw.test function in the R package pegas
246 (Fisher's exact test with 1,000 MCMC replicates) [64]. *P*-values from the Hardy-Weinberg tests
247 were corrected for multiple comparisons using the Benjamini and Hochberg method in the R
248 package sgof [65–67]. The inbreeding coefficient, F_{IS}, was estimated using the R package
249 hierfstat [68].
250
251 *Estimation of effective population size*
252 We estimated contemporary effective population size (N_e) for GLE blue wildebeest using the
253 bias-corrected linkage disequilibrium method [69,70] implemented in NeEstimator version 2.1
254 [71] assuming a random-mating model. 95% confidence intervals for N_e were constructed using
255 the parametric method of Waples [69] and the jackknifing method of Jones et al. [72], which
256 accounts for pseudoreplication resulting from physically linked loci and is recommended for data
257 sets including large numbers of SNPs.
258
259 *Population structure*
260 We explored whether genetic structure is present within the GLE wildebeest population using the
261 model-based clustering approach implemented in STRUCTURE version 2.3.4 [73–76]. We

262 assumed the admixture model and correlated allele frequencies [74,77]. Ten independent runs
263 were performed for each number of genetic clusters tested (K = 1 to K = 4), and each run
264 contained 10,000 burn-in steps and 100,000 MCMC steps. We used STRUCTURE
265 HARVESTER web version 0.6.94 [78,79] to summarize STRUCTURE results, and the best K
266 value was selected based on the log probability of the data given the number of clusters (ln
267 Pr(X|K)) and the Evanno ΔK method [80]. Visualizations of the STRUCTURE output were
268 created using the R package and Shiny app pophelper [81]. We also examined genetic structure
269 using a non-model-based approach by performing a principal components analysis (PCA) in the
270 R package adegenet [62].
271
272 *Demographic history*
273 Using the coalescent simulator fastsimcoal version 2.6 [47] we evaluated five models of
274 historical demographic change: constant population size, expansion, decline, bottleneck, and
275 expansion followed by decline (hereafter "expansion-decline"; Figure 2). Fastsimcoal2 simulates
276 the expected site frequency spectrum (SFS) for a demographic model provided by the user and
277 computes the composite likelihood of the SFS observed from the data given this model. We
278 computed the folded site frequency spectrum from the minor allele frequencies of all sites in
279 1,831 loci (2,946 SNPs and 172,603 monomorphic sites) that passed quality filtering without
280 applying the minor allele frequency filter, as excluding singletons can bias inferences drawn
281 from the site frequency spectrum [82].
282 **Fig. 2. Schematic of the five demographic scenarios modeled in the coalescent simulator**
283 **fastsimcoal2.** For each model, parameters describing effective population size (N) and select
284 times before present (T) were estimated.

285 For each model, we ran 50 replicate simulations, each with randomly selected initial
286 parameter values, to increase the likelihood that the global maximum solution was discovered.
287 Each run included 100,000 coalescent simulations and 40 cycles of Brent's ECM algorithm,
288 which is used to select parameters for the model that optimize the composite likelihood [47]. We
289 provided broad parameter search ranges of 10–100,000 gene copies (haploid N) for all N_e
290 estimates, except $N_{ancestral}$ in the decline and bottleneck models and N_{mid} in the expansion-decline
291 model, which were set to 10–1,000,000 gene copies. The search range for all event time
292 parameters was 10-100,000 generations. The mutation rate was set to 1.7×10^{-8} substitutions per
293 base pair per generation, based on the average mammalian mutation rate (2.22×10^{-9} substitutions
294 per base pair per year) [83] and the generation time of wildebeest (7.5 years) [84]. For each
295 demographic scenario, the replicate with the highest likelihood was retained as the best model.
296 Fastsimcoal2 handles effective population size as the number of gene copies, so N_e was
297 converted to the number of diploid individuals by dividing all estimated N_e parameters by two.
298 Time parameters were converted from number of generations to years before present by
299 multiplying T estimates by a generation time of 7.5 years. We calculated Akaike Information
300 Criterion (AIC) values [85] for the models with the highest maximum composite likelihood for
301 each demographic scenario and compared the demographic models using Akaike weights
302 (AICw) calculated using the akaike.weights function in the qpcR R package [86].
303 In addition to the model-based approach implemented in fastsimcoal2, we also inferred
304 historical changes in population size using the model-independent stairway plot method.
305 Stairway Plot 2 uses a flexible multi-epoch model to estimate population size over different time
306 intervals based on the site frequency spectrum [48,49]. The same folded site frequency spectrum,
307 mutation rate, and generation time used in the fastsimcoal2 analysis were used to generate the

308 stairway plot. Confidence intervals were created based on 200 bootstrapped site frequency
309 spectra drawn from the observed SFS.
310
311 **RESULTS**
312 Sequencing produced ~220 million reads that passed initial Illumina quality filtering, and
313 demultiplexing resulted in an average of 2.2 million reads assigned to each wildebeest. After
314 these reads were filtered for quality and clustered by similarity, 22,483 RAD loci were identified.
315 A similar number of loci aligned to each reference genome: 19,216 (85.5%) of sequences
316 generated at least one BLAST hit to the sheep genome, and 19,267 (85.7%) of loci aligned to the
317 blue wildebeest genome. Eight wildebeest samples were removed due to low sequencing depth
318 (<10 reads per locus), leaving 75 wildebeest that were genotyped. There were 3,417 polymorphic
319 loci that were genotyped in >90% of samples. Many putatively paralogous loci were removed
320 from the dataset, likely the result of the large proportion of repetitive sequence in bovid genomes
321 (~50%) [54,87]. After all quality filtering (Supplementary Table 1), the final dataset included
322 1,730 high-quality polymorphic RAD loci (mean length = 96 bp, mean depth = 355X) that
323 passed a minor allele frequency (MAF) threshold of 0.01, containing 2,921 SNPs. The number of
324 loci that aligned to each chromosome of the sheep genome was correlated with the length of the
325 chromosome (Spearman's $\rho = 0.683$, $P < 0.001$; Supplementary Figure 1), indicating that the
326 dataset contains loci evenly spaced throughout the genome.
327 We estimated genetic diversity and effective population size for GLE blue wildebeest (n
328 = 75) using 1,730 biallelic SNPs, with one SNP randomly drawn from each RAD locus. After
329 correcting for multiple comparisons, no SNPs in the final dataset significantly deviated from
330 Hardy-Weinberg equilibrium ($\alpha = 0.05$). The minor allele frequency per SNP ranged from 0.01

331 to 0.50, with a mean of 0.14 (SD = 0.13). The observed heterozygosity of the SNPs ranged from
332 0 to 0.597, and the average observed heterozygosity of GLE blue wildebeest was 0.204 (SD =
333 0.150; Figure 3). Expected heterozygosity per SNP ranged from 0.013 to 0.504, and the average
334 expected heterozygosity was 0.209 (SD = 0.151). The inbreeding coefficient (F_{IS}) for the
335 population was 0.031 (95% CI: 0.026 – 0.038). The estimated effective population size (N_e) was
336 5,075 (parametric 95% CI = 3,360–10,322; jackknifing 95% CI = 800–∞).

337 **Fig. 3. Expected and observed heterozygosity for 1,730 SNPs genotyped in Greater Liuwa**
338 **Ecosystem blue wildebeest (*n* = 75).** Boxplots show median and interquartile range.

339 We did not detect any genetic population structure within the GLE blue wildebeest. The
340 most likely number of clusters identified using STRUCTURE was $K = 1$ (Supplementary Table
341 2), and for each K value >1 that was tested, almost all individuals were assigned membership to
342 multiple clusters (Figure 4a; Supplementary Figure 2). Principal component analysis also did not
343 show any genetic clustering of subpopulations within the GLE (Figure 4b). Rather, the GLE blue
344 wildebeest seem to compose a single, panmictic population.

345 **Fig. 4. Blue wildebeest show no signs of population subdivision within the Greater Liuwa**
346 **Ecosystem**. (a) Model-based clustering in STRUCTURE (shown are membership coefficients
347 for K=2 clusters for 75 individuals). (b) Principal component analysis (PCA) based on 1,730
348 SNPs.

349 The results of both the model-based fastsimcoal2 analysis and model-independent
350 stairway plot analysis suggest that the GLE blue wildebeest experienced population expansion
351 during the Pleistocene followed by large declines throughout the Late Pleistocene and Holocene.
352 Of the five demographic models simulated in fastsimcoal2 (Figure 2), the expansion-decline
353 model had the highest composite likelihood score and Akaike weight (w_i; Table 1). The

354 parameters of the highest-likelihood expansion-decline model suggest a population increase from
355 N_e=26,800 to N_e=92,700 occurring 635,000 years ago, followed by a population decline to
356 N_e=13,400 occurring 15,480 years ago (Supplementary Table 3). The stairway plot exhibited
357 similar changes in population size as the fastsimcoal2 expansion-decline model (Figure 5), with
358 an increase in population size from N_e=30,000 to N_e=90,000 from 1,000,000-500,000 years ago,
359 followed by a sharp decline to N_e=11,000 from 25,000-3,000 years ago.
360
361 **Table 1. Comparison of likelihood scores and Akaike information criterion (AIC) values**
362 **for the highest likelihood model produced for each demographic scenario tested using the**
363 **coalescent simulator fastsimcoal2.** The best supported model is shown in bold.

Model	**Log likelihood**	***k***	**AIC**	**ΔAIC**	**Akaike weight (w_i)**
Constant size	-11,513.55	1	23,029.10	120.70	0.00
Expansion	-11,514.12	3	23,034.24	125.84	0.00
Decline	-11,463.62	3	22,933.25	24.85	0.00
Bottleneck	-11,462.90	4	22,933.79	25.39	0.00
Expansion-Decline	**-11,449.20**	**5**	**22,908.40**	**0.00**	**1.00**

364
365
366 **Fig. 5 Stairway plot representing inferred changes in effective population size (N_e) over**
367 **time for the Greater Liuwa Ecosystem blue wildebeest population.** The red line shows the
368 median estimated effective population size, the dark grey lines encompass the 75% CI, and the
369 light gray lines contain the 95% CI, determined from 200 bootstrapped site frequency spectrums.

370 **DISCUSSION**

371 Our results show that a single, panmictic blue wildebeest population occupies the GLE,
372 possessing moderate levels of genetic diversity, no evidence of inbreeding, and no genetic
373 population structure. Though relatively few population genomic studies of wild ungulates have
374 measured SNP-based heterozygosity, the level of heterozygosity seen in GLE blue wildebeest
375 (average per-SNP H_o = 0.204) was slightly higher than average per-SNP heterozygosity in
376 another African antelope, the springbok (*Antidorcas marsupialis*; H_o = 0.15) [88], and similar to
377 that seen in pronghorn (*Antilocapra americana*; H_o = 0.21) [89]. Heterozygosity in GLE
378 wildebeest was slightly lower than that found in African forest elephants (*Loxodonta cyclotis*; H_o
379 = 0.27) [90], although the elephant value was averaged over multiple sampling locations. One
380 other study has reported per-SNP heterozygosity for reduced-representation genomic data from
381 blue wildebeest (~20,000 SNPs generated using DArT-seq) [91]. From their dataset generated
382 for wildebeest from a South African private game ranch, van Deventer et al. [91] found a mean
383 minor allele frequency (0.19) and average observed heterozygosity (0.19) similar to those of the
384 GLE blue wildebeest. However, in the South African population, observed heterozygosity was
385 significantly lower than expected heterozygosity (0.27), potentially a sign of inbreeding that was
386 not seen in the GLE blue wildebeest.

387 While direct comparison to other previously published studies of genetic variation in blue
388 wildebeest is more challenging, especially those that utilized allozymes, microsatellites, and
389 mitochondrial DNA, the GLE blue wildebeest seem to have relatively greater genetic diversity
390 than some previously studied populations. Researchers found low allozyme polymorphism and
391 low heterozygosity in wildebeest from Tanzania and Kenya [92], and low mtDNA nucleotide
392 diversity [42] and allozyme heterozygosity [43] in South African wildebeest. Many of these early

393 studies focused on smaller, more heavily managed wildebeest populations that likely were
394 experiencing founder effects resulting from translocations of individuals from one reserve to
395 another. In contrast, wildebeest in the GLE are free-ranging and do not have a history of
396 translocations or intensive management. In a recent study of wildebeest populations throughout
397 their range using whole-genome data, Liu et al. [39] found lower genome-wide heterozygosity
398 estimates and more runs of homozygosity (a sign of past inbreeding) in nonmigratory wildebeest
399 populations compared to migratory ones. Though the GLE wildebeest numbers declined
400 drastically in the early 2000's and the migration no longer extends into Angola, it does not seem
401 that these changes have resulted in low genetic diversity in Liuwa compared to other
402 populations.

403 The GLE blue wildebeest exhibited no signs of inbreeding. Though F_{IS} was significantly
404 greater than zero (0.033; 95% CI: 0.026 – 0.039), indicating a slight excess of homozygosity, this
405 low value does not indicate extensive nonrandom mating in the population. Similar values of the
406 inbreeding coefficient have been seen in springbok (F_{IS} = 0.018 – 0.032) from several
407 populations in South Africa [88]. While the GLE blue wildebeest population experienced
408 significant declines in the early 2000's [34], it seems these declines were not great enough and
409 did not last long enough (occurring over a few generations) to lead to inbreeding and reduction
410 of genetic diversity in the population. We also found no evidence of population structure using
411 either STRUCTURE or PCA, indicating that a single, panmictic wildebeest population inhabits
412 the GLE. Visual observation and GPS tracking of collared wildebeest have found that the GLE
413 wildebeest spend the wet season in a concentrated area in the southern portion of the park [33],
414 and our genetic results corroborate that there is likely no spatial segregation of individuals during
415 breeding.

416 Our estimate of the current effective population size (N_e), the size of an idealized
417 population that would experience the same amount of genetic drift as the population being
418 studied [93], was 5,075 (95% CI = 3,360–10,322). Estimating a population's effective size is
419 important for conservation, because a population with low N_e could lose genetic diversity faster
420 than expected based on its census population size (N). The effective population size estimated for
421 wildebeest in the GLE is 11% of the total estimated population size determined using aerial
422 surveys in 2013 (N = 46,000) [35]—an effective to census population size ratio (N_e/N) similar to
423 estimates for many comparable mammals. Reviews have found the average N_e/N ratio in wildlife
424 to be 0.10-0.14 [94,95]. In African buffalo, another large, highly mobile ungulate with a
425 promiscuous mating system, researchers have estimated N_e/N ratios ranging from 0.10 to 0.20
426 [96]. When also considering the moderate level of heterozygosity and low inbreeding coefficient
427 for the Liuwa population, it seems unlikely that this estimate of current effective population size
428 is indicative of a loss in genetic diversity after the population decline in the early 2000's. Very
429 recent population declines can actually increase the N_e/N ratio, because census population size
430 decreases faster than the timescale required for N_e to be reduced by a loss of genetic diversity
431 [37,38,95]. By comparison, LaCava et al. [89] estimated a very low N_e/N ratio of 0.01-0.02 for
432 pronghorn (*Antilocaptra americana*), a North American ungulate that, in addition to having a
433 polygynous mating system, experienced precipitous declines over a century ago.
434 Using both model-based and model-independent methods, we detected signatures of
435 population expansion followed by decline in the site frequency spectrum of GLE blue
436 wildebeest. Both the highest-likelihood expansion-decline fastsimcoal2 model and the stairway
437 plot inferred a threefold increase in population size during the Middle Pleistocene, followed by
438 an ~87% reduction in population size during the Late Pleistocene and early Holocene. Evidence

439 of Pleistocene population expansions followed by Holocene declines has been found in a number
440 of other African mammal species using genetic data, including African buffalo [23,24],
441 hippopotamus [26,27], African elephant [25,97], and savannah baboon [98]. In a comparative
442 study of ruminant whole genomes, including 26 African species, Chen et al. [54] found using the
443 pairwise sequentially Markovian coalescent (PSMC) method that most of the African species
444 shared a similar demographic history of population expansion followed by decline in the late
445 Pleistocene. Similarly, Liu et al. [39] used PSMC to infer effective population size over time for
446 the five blue wildebeest subspecies, and the demographic history inferred for the brindled
447 wildebeest (which did not include any individuals from the GLE) is very similar to the results of
448 our stairway plot analysis in both the timing of the expansion and decline and the effective
449 populations sizes inferred.

450 Two primary explanations have been proposed to explain the population declines in
451 African ungulates during the late Pleistocene and early Holocene: climatic change and
452 anthropogenic impacts [99]. Ice core records and other paleontological data suggest that Africa
453 experienced large fluctuations in precipitation during the late Pleistocene and early Holocene,
454 with extensive periods of drought [28–30]. Such climatic changes could have a profound impact
455 on wildebeest, as modern-day wildebeest populations have fluctuated in response to drought [19]
456 and wildebeest migration is at least partially driven by changes in rainfall and forage availability
457 [4]. However, others have argued that climatic changes in the late Pleistocene were no more
458 extreme than those occurring earlier in the epoch, and thus do not alone explain population
459 declines and extinctions [99]. Human population growth and the advent of pastoralism during the
460 Neolithic revolution may have increased pressures on ungulate populations already stressed by
461 drought, leading to the observed declines [23,54]. Past population declines in the face of climatic

462 changes and intensified human activity reflect the modern-day pressures faced by blue
463 wildebeest, as habitat destruction, overhunting, and climate change all threaten the species today.
464 Our results show that—despite recent declines in population size and the disruption of
465 migration to Angola—the GLE blue wildebeest population does not seem to have experienced
466 recent reductions in genetic diversity or increased inbreeding. The ecosystem restoration efforts
467 implemented in the GLE likely allowed the wildebeest population to increase before the
468 bottleneck became severe enough to result in detectable reductions in genetic diversity.
469 However, wildebeest continue to face threats of habitat destruction, obstruction of migration
470 routes from fencing, and climate change, and continued genetic monitoring could detect whether
471 these impacts are influencing genetic diversity in the GLE in the future. This is especially
472 important given the evidence that blue wildebeest population size drastically decreased during
473 past periods of climate change and anthropogenic pressure in the late Pleistocene and early
474 Holocene.
475 Future sampling and genomic analysis of wildebeest from Kafue National Park in Zambia
476 could help to elucidate patterns of connectivity or differentiation between wildebeest in the GLE
477 and those in a neighboring population that is also of conservation significance. The Zambezi
478 River, which separates these two protected areas and currently acts as a barrier, may have
479 historically prevented gene flow, leading to genetic differentiation between these populations.
480 Analysis of four wildebeest genomes from Kafue by Liu et al. [39] suggested that the Kafue
481 population was genetically distinct from more southern brindled wildebeest populations, but the
482 relationship between the Kafue and GLE populations remains unknown. Understanding patterns
483 of genetic differentiation between GLE blue wildebeest and those in Kafue National Park would
484 have important implications for future management decisions such as translocations between

485 these populations. Our study provides a baseline understanding of genetic diversity and long-
486 term demographic history for Africa's second largest migratory blue wildebeest population,
487 which will assist the development of effective conservation plans for the species as wildebeest
488 face threats of habitat destruction and overhunting.

REFERENCES

1. Fryxell JM, Sinclair ARE. Causes and consequences of migration by large herbivores. Trends in Ecology & Evolution. 1988;3: 237–241. doi:10.1016/0169-5347(88)90166-8
2. Wilmshurst JF, Fryxell JM, Farm BP, Sinclair ARE, Henschel CP. Spatial distribution of Serengeti wildebeest in relation to resources. 1999;77: 10.
3. Boone RB, Thirgood SJ, Hopcraft JGC. Serengeti wildebeest migratory patterns modeled from rainfall and new vegetation growth. Ecology. 2006;87: 1987–1994. doi:10.2307/20069184
4. Holdo RM, Holt RD, Fryxell JM. Opposing rainfall and plant nutritional gradients best explain the wildebeest migration in the Serengeti. The American Naturalist. 2009;173: 431–445. doi:10.1086/597229
5. McNaughton SJ. Serengeti migratory wildebeest: facilitation of energy flow by grazing. Science. 1976;191: 92–94. doi:10.1126/science.191.4222.92
6. Holdo RM, Holt RD, Coughenour MB, Ritchie ME. Plant productivity and soil nitrogen as a function of grazing, migration and fire in an African savanna. Journal of Ecology. 2007;95: 115–128. doi:10.1111/j.1365-2745.2006.01192.x
7. Estes RD, Raghunathan TE, Vleck DV. The impact of horning by wildebeest on woody vegetation of the Serengeti ecosystem. The Journal of Wildlife Management. 2008;72: 1572–1578. doi:10.2193/2008-105
8. Sinclair ARE. Mammal population regulation, keystone processes and ecosystem dynamics. Philos Trans R Soc Lond B Biol Sci. 2003;358: 1729–1740. doi:10.1098/rstb.2003.1359
9. Hayward MW, Kerley GIH. Prey preferences of the lion (Panthera leo). Journal of Zoology. 2005;267: 309–322. doi:10.1017/S0952836905007508

10. Hayward MW. Prey preferences of the spotted hyaena (Crocuta crocuta) and degree of dietary overlap with the lion (Panthera leo). Journal of Zoology. 2006;270: 606–614. doi:10.1111/j.1469-7998.2006.00183.x

11. Creel S, Dröge E, M'soka J, Smit D, Becker M, Christianson D, et al. The relationship between direct predation and antipredator responses: a test with multiple predators and multiple prey. Ecology. 2017;98: 2081–2092. doi:10.1002/ecy.1885

12. Dröge E, Creel S, Becker MS, M'soka J. Spatial and temporal avoidance of risk within a large carnivore guild. Ecology and Evolution. 2017;7: 189–199. doi:10.1002/ece3.2616

13. Lee DE, Kissui BM, Kiwango YA, Bond ML. Migratory herds of wildebeests and zebras indirectly affect calf survival of giraffes. Ecology and Evolution. 2016;6: 8402–8411. doi:10.1002/ece3.2561

14. Estes R. The gnu's world: Serengeti wildebeest ecology and life history. Berkeley: University of California Press; 2014.

15. Serneels S, Lambin EF. Impact of land-use changes on the wildebeest migration in the northern part of the Serengeti-Mara Ecosystem. Journal of Biogeography. 2001;28: 391–407. doi:10.2307/2656203

16. Homewood K, Lambin EF, Coast E, Kariuki A, Kikula I, Kivelia J, et al. Long-term changes in Serengeti-Mara wildebeest and land cover: pastoralism, population, or policies? PNAS. 2001;98: 12544–12549. doi:10.1073/pnas.221053998

17. Whyte CSJ, Joubert IJ. Blue wildebeest population trends in the Kruger National Park and the effects of fencing. South African Journal of Wildlife Research - 24-month delayed open access. 1988;18: 78–87.

534 18. Holdo RM, Fryxell JM, Sinclair ARE, Dobson A, Holt RD. Predicted impact of barriers to
535 migration on the Serengeti Wildebeest population. PLoS ONE. 2011;6: e16370.
536 doi:10.1371/journal.pone.0016370
537 19. Mduma SAR, Sinclair ARE, Hilborn R. Food regulates the Serengeti wildebeest: a 40-year
538 record. Journal of Animal Ecology. 1999;68: 1101–1122. doi:10.1046/j.1365-
539 2656.1999.00352.x
540 20. Thirgood S, Mosser A, Tham S, Hopcraft G, Mwangomo E, Mlengeya T, et al. Can parks
541 protect migratory ungulates? The case of the Serengeti wildebeest. Animal Conservation.
542 2004;7: 113–120. doi:10.1017/S1367943004001404
543 21. Harris G, Thirgood S, Hopcraft JGC, Cromsight JPGM, Berger J. Global decline in
544 aggregated migrations of large terrestrial mammals. Endangered Species Research. 2009;7:
545 55–76. doi:10.3354/esr00173
546 22. Heller R, Lorenzen ED, Okello JBA, Masembe C, Siegismund HR. Mid-Holocene decline in
547 African buffalos inferred from Bayesian coalescent-based analyses of microsatellites and
548 mitochondrial DNA. Molecular Ecology. 2008;17: 4845–4858. doi:10.1111/j.1365-
549 294X.2008.03961.x
550 23. Heller R, Brüniche-Olsen A, Siegismund HR. Cape buffalo mitogenomics reveals a
551 Holocene shift in the African human–megafauna dynamics. Molecular Ecology. 2012;21:
552 3947–3959. doi:10.1111/j.1365-294X.2012.05671.x
553 24. de Jager D, Glanzmann B, Möller M, Hoal E, van Helden P, Harper C, et al. High diversity,
554 inbreeding and a dynamic Pleistocene demographic history revealed by African buffalo
555 genomes. Sci Rep. 2021;11: 4540. doi:10.1038/s41598-021-83823-8

25. Okello JBA, Wittemyer G, Rasmussen HB, Arctander P, Nyakaana S, Douglas-Hamilton I, et al. Effective population size dynamics reveal impacts of historic climatic events and recent anthropogenic pressure in African elephants. Molecular Ecology. 2008;17: 3788–3799. doi:10.1111/j.1365-294X.2008.03871.x

26. Okello JBA, Nyakaana S, Masembe C, Siegismund HR, Arctander P. Mitochondrial DNA variation of the common hippopotamus: evidence for a recent population expansion. Heredity. 2005;95: 206–215. doi:10.1038/sj.hdy.6800711

27. Stoffel C, Dufresnes C, Okello JBA, Noirard C, Joly P, Nyakaana S, et al. Genetic consequences of population expansions and contractions in the common hippopotamus (Hippopotamus amphibius) since the Late Pleistocene. Molecular Ecology. 2015;24: 2507–2520. doi:10.1111/mec.13179

28. Thompson LG, Mosley-Thompson E, Davis ME, Henderson KA, Brecher HH, Zagorodnov VS, et al. Kilimanjaro ice core records: evidence of Holocene climate change in tropical Africa. Science. 2002;298: 589–593. doi:10.1126/science.1073198

29. Marchant R, Hooghiemstra H. Rapid environmental change in African and South American tropics around 4000 years before present: a review. Earth-Science Reviews. 2004;66: 217–260. doi:10.1016/j.earscirev.2004.01.003

30. Kiage LM, Liu K. Late Quaternary paleoenvironmental changes in East Africa: a review of multiproxy evidence from palynology, lake sediments, and associated records. Progress in Physical Geography. 2006;30: 633–658. doi:10.1177/0309133306071146

31. Durant SM, Becker MS, Creel S, Bashir S, Dickman AJ, Beudels-Jamar RC, et al. Developing fencing policies for dryland ecosystems. Journal of Applied Ecology. 2015;52: 544–551. doi:10.1111/1365-2664.12415

32. M'soka J, Creel S, Becker MS, Murdoch JD. Ecological and anthropogenic effects on the density of migratory and resident ungulates in a human-inhabited protected area. Afr J Ecol. 2017;55: 618–631. doi:10.1111/aje.12398

33. Watson F, Becker MS, Smit D, Droge E, Mukula T, Martens S, et al. Predation strongly limits demography of a keystone migratory herbivore in a recovering transfrontier ecosystem. Ecology and Evolution. 2022;12: e9414. doi:10.1002/ece3.9414

34. Nyirenda VR, Nkhata BA. Collaborative governance and benefit sharing in Liuwa Plain National Park, western Zambia. PARKS. 2013;19: 103–114. doi:10.2305/IUCN.CH.2013.PARKS-19-1.VRN.en

35. African Parks Network. Aerial survey confirms substantial increase in important indicator species in Liuwa. 2013 [cited 18 Jun 2024]. Available: https://www.african-parks.org/newsroom/press-releases/aerial-survey-confirms-substantial-increase-Important-indicator-species-liuwa

36. Dröge E, Creel S, Becker M, Christianson D, M'Soka J, Watson F. Response of wildebeest (Connochaetes taurinus) movements to spatial variation in long term risks from a complete predator guild. Biological Conservation. 2019;233: 139–151. doi:10.1016/j.biocon.2019.02.031

37. Dedato MN, Robert C, Taillon J, Shafer ABA, Côté SD. Demographic history and conservation genomics of caribou (Rangifer tarandus) in Québec. Evolutionary Applications. 2022;15: 2043–2053. doi:10.1111/eva.13495

38. Wootton E, Robert C, Taillon J, Côté SD, Shafer ABA. Genomic health is dependent on long-term population demographic history. Molecular Ecology. 2023;32: 1943–1954. doi:10.1111/mec.16863

602 39. Liu X, Lin L, Sinding M-HS, Bertola LD, Hanghøj K, Quinn L, et al. Introgression and
603 disruption of migration routes have shaped the genetic integrity of wildebeest populations.
604 Nat Commun. 2024;15: 2921. doi:10.1038/s41467-024-47015-y
605 40. Allendorf FW, Hohenlohe PA, Luikart G. Genomics and the future of conservation genetics.
606 2010.
607 41. Funk WC, McKay JK, Hohenlohe PA, Allendorf FW. Harnessing genomics for delineating
608 conservation units. Trends in Ecology & Evolution. 2012;27: 489–496.
609 doi:10.1016/j.tree.2012.05.012
610 42. Corbet SW, Robinson TJ. Genetic divergence in South African wildebeest: comparative
611 cytogenetics and analysis of mitochondrial DNA. J Hered. 1991;82: 447–452.
612 doi:10.1093/oxfordjournals.jhered.a111126
613 43. Grobler JP, Van der Bank FH. Genetic variability in South African blue wildebeest
614 (*Connochaetes taurinus*). Comparative Biochemistry and Physiology Part B: Comparative
615 Biochemistry. 1993;106: 755–759. doi:10.1016/0305-0491(93)90159-3
616 44. Corbet SW, Grant WS, Robinson TJ. Genetic divergence in South African wildebeest:
617 analysis of allozyme variability. J Hered. 1994;85: 479–483.
618 doi:10.1093/oxfordjournals.jhered.a111504
619 45. Arctander P, Johansen C, Coutellec-Vreto MA. Phylogeography of three closely related
620 African bovids (tribe Alcelaphini). Mol Biol Evol. 1999;16: 1724–1739.
621 doi:10.1093/oxfordjournals.molbev.a026085
622 46. Grobler JP, Hartl GB, Grobler N, Kotze A, Botha K, Tiedemann R. The genetic status of an
623 isolated black wildebeest (*Connochaetes gnou*) population from the Abe Bailey Nature
624 Reserve, South Africa: Microsatellite data on a putative past hybridization with blue

625 wildebeest (*C. taurinus*). Mammalian Biology - Zeitschrift für Säugetierkunde. 2005;70:
626 35–45. doi:10.1078/1616-5047-00174
627 47. Excoffier L, Dupanloup I, Huerta-Sánchez E, Sousa VC, Foll M. Robust demographic
628 inference from genomic and SNP data. PLOS Genetics. 2013;9: e1003905.
629 doi:10.1371/journal.pgen.1003905
630 48. Liu X, Fu Y-X. Exploring population size changes using SNP frequency spectra. Nat Genet.
631 2015;47: 555–559. doi:10.1038/ng.3254
632 49. Liu X, Fu Y-X. Stairway Plot 2: demographic history inference with folded SNP frequency
633 spectra. Genome Biology. 2020;21: 280. doi:10.1186/s13059-020-02196-9
634 50. DaCosta JM, Sorenson MD. Amplification Biases and Consistent Recovery of Loci in a
635 Double-Digest RAD-seq Protocol. PLOS ONE. 2014;9: e106713.
636 doi:10.1371/journal.pone.0106713
637 51. Andrews S. FastQC: a quality control tool for high throughput sequence data. In: Babraham
638 Bioinformatics [Internet]. 2010. Available:
639 https://www.bioinformatics.babraham.ac.uk/projects/fastqc/
640 52. Edgar RC. Search and clustering orders of magnitude faster than BLAST. Bioinformatics.
641 2010;26: 2460–2461. doi:10.1093/bioinformatics/btq461
642 53. Altschul SF, Gish W, Miller W, Myers EW, Lipman DJ. Basic local alignment search tool. J
643 Mol Biol. 1990;215: 403–410. doi:10.1016/S0022-2836(05)80360-2
644 54. Chen L, Qiu Q, Jiang Y, Wang K, Lin Z, Li Z, et al. Large-scale ruminant genome
645 sequencing provides insights into their evolution and distinct traits. Science. 2019;364:
646 eaav6202. doi:10.1126/science.aav6202

647 55. Edgar RC. MUSCLE: multiple sequence alignment with high accuracy and high throughput.
648 Nucleic Acids Res. 2004;32: 1792–1797. doi:10.1093/nar/gkh340
649 56. Wickham H. tidyverse: Easily Install and Load the "Tidyverse". In: R package version
650 1.2.1. [Internet]. 2017. Available: https://CRAN.R-project.org/package=tidyverse
651 57. R Core Team. R: A language and environment for statistical computing. Vienna, Austria: R
652 Foundation for Statistical Computing; 2024. Available: https://www.R-project.org/
653 58. O'Leary SJ, Puritz JB, Willis SC, Hollenbeck CM, Portnoy DS. These aren't the loci you're
654 looking for: Principles of effective SNP filtering for molecular ecologists. Molecular
655 Ecology. 2018;27: 3193–3206. doi:10.1111/mec.14792
656 59. Emerson KJ, Merz CR, Catchen JM, Hohenlohe PA, Cresko WA, Bradshaw WE, et al.
657 Resolving postglacial phylogeography using high-throughput sequencing. PNAS.
658 2010;107: 16196–16200. doi:10.1073/pnas.1006538107
659 60. Willis SC, Hollenbeck CM, Puritz JB, Gold JR, Portnoy DS. Haplotyping RAD loci: an
660 efficient method to filter paralogs and account for physical linkage. Molecular Ecology
661 Resources. 2017;17: 955–965. doi:10.1111/1755-0998.12647
662 61. Lischer HEL, Excoffier L. PGDSpider: an automated data conversion tool for connecting
663 population genetics and genomics programs. Bioinformatics. 2012;28: 298–299.
664 doi:10.1093/bioinformatics/btr642
665 62. Jombart T. adegenet: a R package for the multivariate analysis of genetic markers.
666 Bioinformatics. 2008;24: 1403–1405. doi:10.1093/bioinformatics/btn129
667 63. Jombart T, Ahmed I. adegenet 1.3-1: new tools for the analysis of genome-wide SNP data.
668 Bioinformatics. 2011;27: 3070–3071. doi:10.1093/bioinformatics/btr521

669 64. Paradis E. pegas: an R package for population genetics with an integrated–modular
670 approach. Bioinformatics. 2010;26: 419–420. doi:10.1093/bioinformatics/btp696
671 65. Benjamini Y, Hochberg Y. Controlling the false discovery rate: a practical and powerful
672 approach to multiple testing. Journal of the Royal Statistical Society Series B
673 (Methodological). 1995;57: 289–300.
674 66. Conde IC, Alvarez J de U. sgof: multiple hypothesis testing. In: R package version 2.3
675 [Internet]. 2016. Available: https://CRAN.R-project.org/package=sgof
676 67. White T, van der Ende J, Nichols TE. Beyond Bonferroni revisited: concerns over inflated
677 false positive research findings in the fields of conservation genetics, biology, and
678 medicine. Conserv Genet. 2019;20: 927–937. doi:10.1007/s10592-019-01178-0
679 68. Goudet J. hierfstat, a package for r to compute and test hierarchical F-statistics. Molecular
680 Ecology Notes. 2005;5: 184–186. doi:10.1111/j.1471-8286.2004.00828.x
681 69. Waples RS. A bias correction for estimates of effective population size based on linkage
682 disequilibrium at unlinked gene loci. Conserv Genet. 2006;7: 167. doi:10.1007/s10592-005-
683 9100-y
684 70. Waples RS, Do C. ldne: a program for estimating effective population size from data on
685 linkage disequilibrium. Mol Ecol Resour. 2008;8: 753–756. doi:10.1111/j.1755-
686 0998.2007.02061.x
687 71. Do C, Waples RS, Peel D, Macbeth GM, Tillett BJ, Ovenden JR. NeEstimator v2: re-
688 implementation of software for the estimation of contemporary effective population size
689 (Ne) from genetic data. Mol Ecol Resour. 2014;14: 209–214. doi:10.1111/1755-0998.12157

690 72. Jones AT, Ovenden JR, Wang Y-G. Improved confidence intervals for the linkage
691 disequilibrium method for estimating effective population size. Heredity (Edinb). 2016;117:
692 217–223. doi:10.1038/hdy.2016.19
693 73. Pritchard JK, Stephens M, Donnelly P. Inference of population structure using multilocus
694 genotype data. Genetics. 2000;155: 945–959.
695 74. Falush D, Stephens M, Pritchard JK. Inference of population structure using multilocus
696 genotype data: linked loci and correlated allele frequencies. Genetics. 2003;164: 1567–
697 1587.
698 75. Falush D, Stephens M, Pritchard JK. Inference of population structure using multilocus
699 genotype data: dominant markers and null alleles. Molecular Ecology Notes. 2007;7: 574–
700 578. doi:10.1111/j.1471-8286.2007.01758.x
701 76. Hubisz MJ, Falush D, Stephens M, Pritchard JK. Inferring weak population structure with
702 the assistance of sample group information. Molecular Ecology Resources. 2009;9: 1322–
703 1332. doi:10.1111/j.1755-0998.2009.02591.x
704 77. Porras-Hurtado L, Ruiz Y, Santos C, Phillips C, Carracedo Á, Lareu MV. An overview of
705 STRUCTURE: applications, parameter settings, and supporting software. Front Genet.
706 2013;4. doi:10.3389/fgene.2013.00098
707 78. Earl DA, vonHoldt BM. STRUCTURE HARVESTER: a website and program for
708 visualizing STRUCTURE output and implementing the Evanno method. Conservation
709 Genet Resour. 2012;4: 359–361. doi:10.1007/s12686-011-9548-7
710 79. Earl D. Structure Harvester Web v0.6.94. 2014. Available:
711 http://taylor0.biology.ucla.edu/structureHarvester/

712 80. Evanno G, Regnaut S, Goudet J. Detecting the number of clusters of individuals using the
713 software STRUCTURE: a simulation study. Molecular Ecology. 2005;14: 2611–2620.
714 doi:10.1111/j.1365-294X.2005.02553.x
715 81. Francis RM. pophelper: an R package and web app to analyse and visualize population
716 structure. Molecular Ecology Resources. 2017;17: 27–32. doi:10.1111/1755-0998.12509
717 82. Brumfield RT, Beerli P, Nickerson DA, Edwards SV. The utility of single nucleotide
718 polymorphisms in inferences of population history. Trends in Ecology & Evolution.
719 2003;18: 249–256. doi:10.1016/S0169-5347(03)00018-1
720 83. Kumar S, Subramanian S. Mutation rates in mammalian genomes. Proc Natl Acad Sci U S
721 A. 2002;99: 803–808. doi:10.1073/pnas.022629899
722 84. IUCN. Connochaetes taurinus: IUCN SSC antelope specialist group: The IUCN red list of
723 threatened species 2008. International Union for Conservation of Nature; 2008.
724 doi:10.2305/IUCN.UK.2008.RLTS.T5229A11120316.en
725 85. Akaike H. A new look at the statistical model identification. IEEE Trans Automat Contr.
726 1974;19: 716–723. doi:10.1109/TAC.1974.1100705
727 86. Ritz C, Spiess A-N. qpcR: an R package for sigmoidal model selection in quantitative real-
728 time polymerase chain reaction analysis. Bioinformatics. 2008;24: 1549–1551.
729 doi:10.1093/bioinformatics/btn227
730 87. Adelson DL, Raison JM, Edgar RC. Characterization and distribution of retrotransposons
731 and simple sequence repeats in the bovine genome. PNAS. 2009;106: 12855–12860.
732 doi:10.1073/pnas.0901282106

733 88. Coetzer WG, Grobler JP. Genetic variation among different springbok (Antidorcas
734 marsupialis) colour variants. Mammalian Biology. 2019;99: 42–53.
735 doi:10.1016/j.mambio.2019.10.006
736 89. LaCava MEF, Gagne RB, Stowell SML, Gustafson KD, Buerkle CA, Knox L, et al.
737 Pronghorn population genomics show connectivity in the core of their range. J Mammal.
738 2020;101: 1061–1071. doi:10.1093/jmammal/gyaa054
739 90. Bourgeois S, Senn H, Kaden J, Taggart JB, Ogden R, Jeffery KJ, et al. Single-nucleotide
740 polymorphism discovery and panel characterization in the African forest elephant. Ecology
741 and Evolution. 2018;8: 2207–2217. doi:10.1002/ece3.3854
742 91. van Deventer R, Rhode C, Marx M, Roodt-Wilding R. The development of genome-wide
743 single nucleotide polymorphisms in blue wildebeest using the DArTseq platform.
744 Genomics. 2020;112: 3455–3464. doi:10.1016/j.ygeno.2020.04.032
745 92. Georgiadis NJ, Kat PW, Oketch H, Patton J. Allozyme divergence within the Bovidae.
746 Evolution. 1990;44: 2135–2149. doi:10.1111/j.1558-5646.1990.tb04317.x
747 93. Wright S. Evolution in Mendelian populations. Genetics. 1931;16: 97–159.
748 94. Frankham R. Relationship of genetic variation to population size in wildlife. Conservation
749 Biology. 1996;10: 1500–1508. doi:10.1046/j.1523-1739.1996.10061500.x
750 95. Palstra FP, Ruzzante DE. Genetic estimates of contemporary effective population size: what
751 can they tell us about the importance of genetic stochasticity for wild population
752 persistence? Molecular Ecology. 2008;17: 3428–3447. doi:10.1111/j.1365-
753 294X.2008.03842.x

96. O'Ryan C, Harley EH, Bruford MW, Beaumont M, Wayne RK, Cherry MI. Microsatellite analysis of genetic diversity in fragmented South African buffalo populations. Animal Conservation. 1998;1: 85–94. doi:10.1111/j.1469-1795.1998.tb00015.x

97. Palkopoulou E, Lipson M, Mallick S, Nielsen S, Rohland N, Baleka S, et al. A comprehensive genomic history of extinct and living elephants. Proceedings of the National Academy of Sciences. 2018;115: E2566–E2574. doi:10.1073/pnas.1720554115

98. Storz JF, Beaumont MA, Alberts SC. Genetic evidence for long-term population decline in a savannah-dwelling primate: inferences from a hierarchical bayesian model. Molecular Biology and Evolution. 2002;19: 1981–1990. doi:10.1093/oxfordjournals.molbev.a004022

99. Barnosky AD, Koch PL, Feranec RS, Wing SL, Shabel AB. Assessing the causes of late Pleistocene extinctions on the continents. Science. 2004;306: 70–75. doi:10.1126/science.1101476

767 **Supporting Information Captions**

768 **Figure S1. Correlation between the number of RAD loci that aligned to each chromosome**
769 **of the domestic sheep (*Ovis aries*) reference genome and the length of the chromosome.**
770 Linear regression line is shown in grey.

771 **Figure S2. Structure plots for 75 wildebeest from the Greater Liuwa Ecosystem based on**
772 **1,730 SNPs assuming *K*=2, *K*=3, and *K*=4 clusters.** None of these *K* values had a higher
773 likelihood than *K*=1, and the assignment of most individuals to multiple clusters indicates that
774 there is no genetic population structure within the GLE.

775 **Table S1. Number of putative RAD loci remaining after each step of the quality filtering**
776 **protocol.** Data is presented separately for loci aligned to the domestic sheep (*Ovis aries*) or blue
777 wildebeest (*Connochaetes taurinus*) reference genomes. Loci aligned to the wildebeest genome
778 were used for downstream analyses.

779 **Table S2. Statistics obtained from Structure Harvester used to determine the optimal**
780 **number of genetic clusters for wildebeest within the Greater Liuwa Ecosystem.** For each *K*
781 value (number of genetic clusters assumed in the model), we report the number of replicates,
782 mean and standard deviation log probability of the data given the number of clusters, and Evanno
783 statistic, ΔK.

784 **Table S3. Parameter estimates from the highest likelihood model for each demographic**
785 **scenario tested in fastsimcoal2.** Parameters describe effective population size (*N*) or the time a
786 demographic event occurred (*T*) in years before present. Estimates have been rounded to the
787 nearest hundred. The model with the highest support is shown in bold.

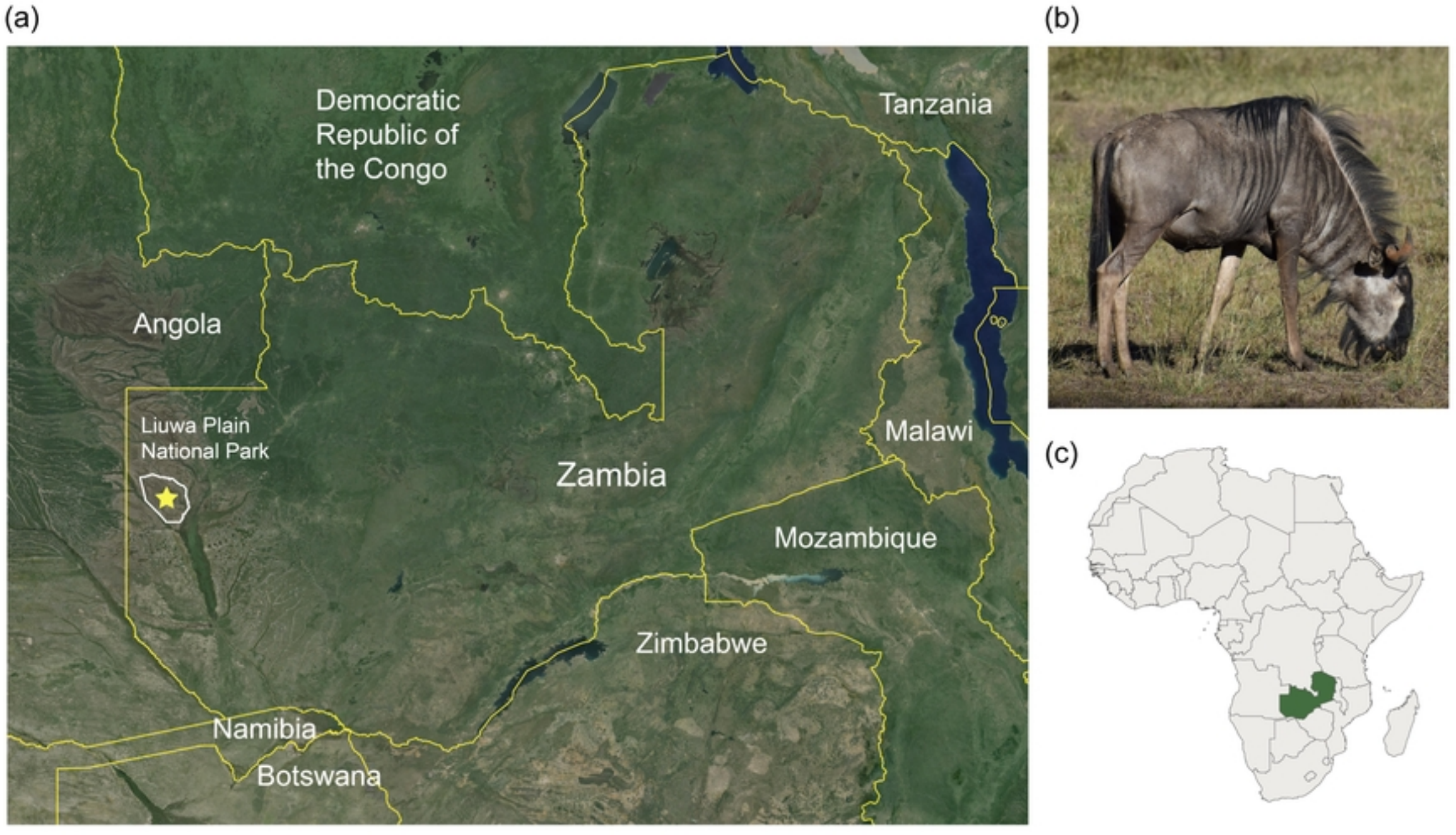
(a)
Democratic
Republic of
the Congo
Tanzania
Angola
Liuwa Plain
National Park
Zambia
Malawi
Mozambique
Zimbabwe
Namibia
Botswana
(b)
(c)

Figure 1

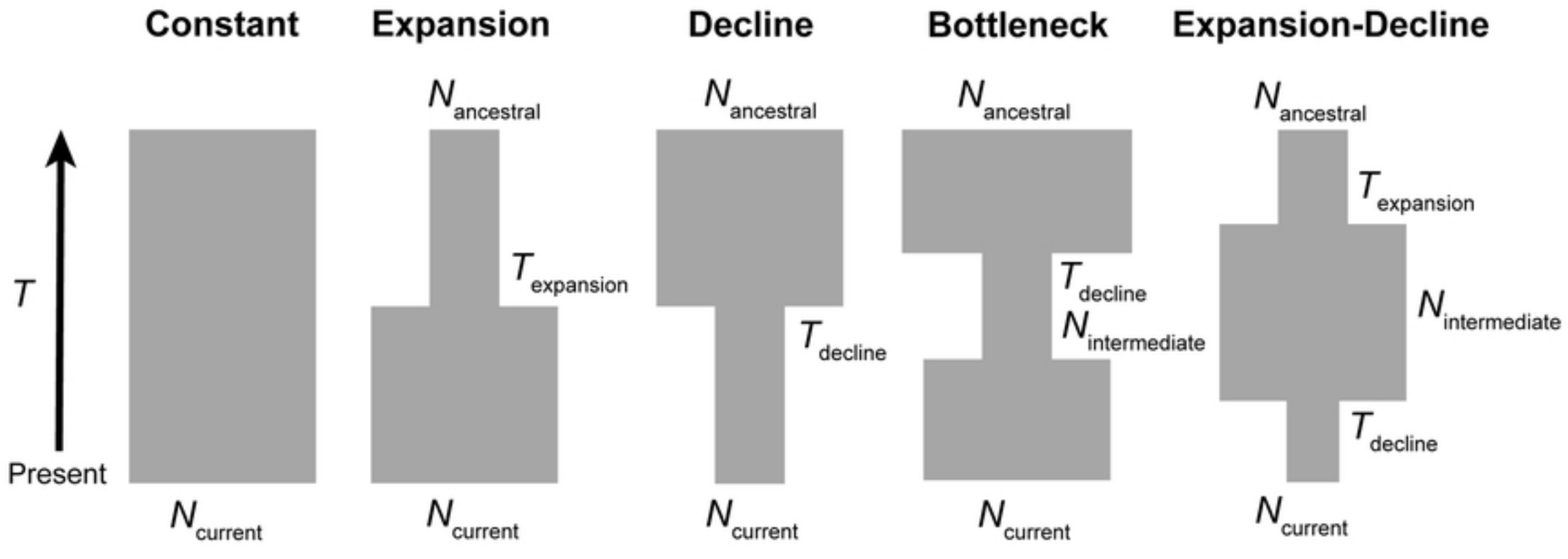
Constant
Expansion
Decline
Bottleneck
Expansion-Decline
T
Present
N ancestral
N current
T expansion
T decline
N intermediate

Figure 2

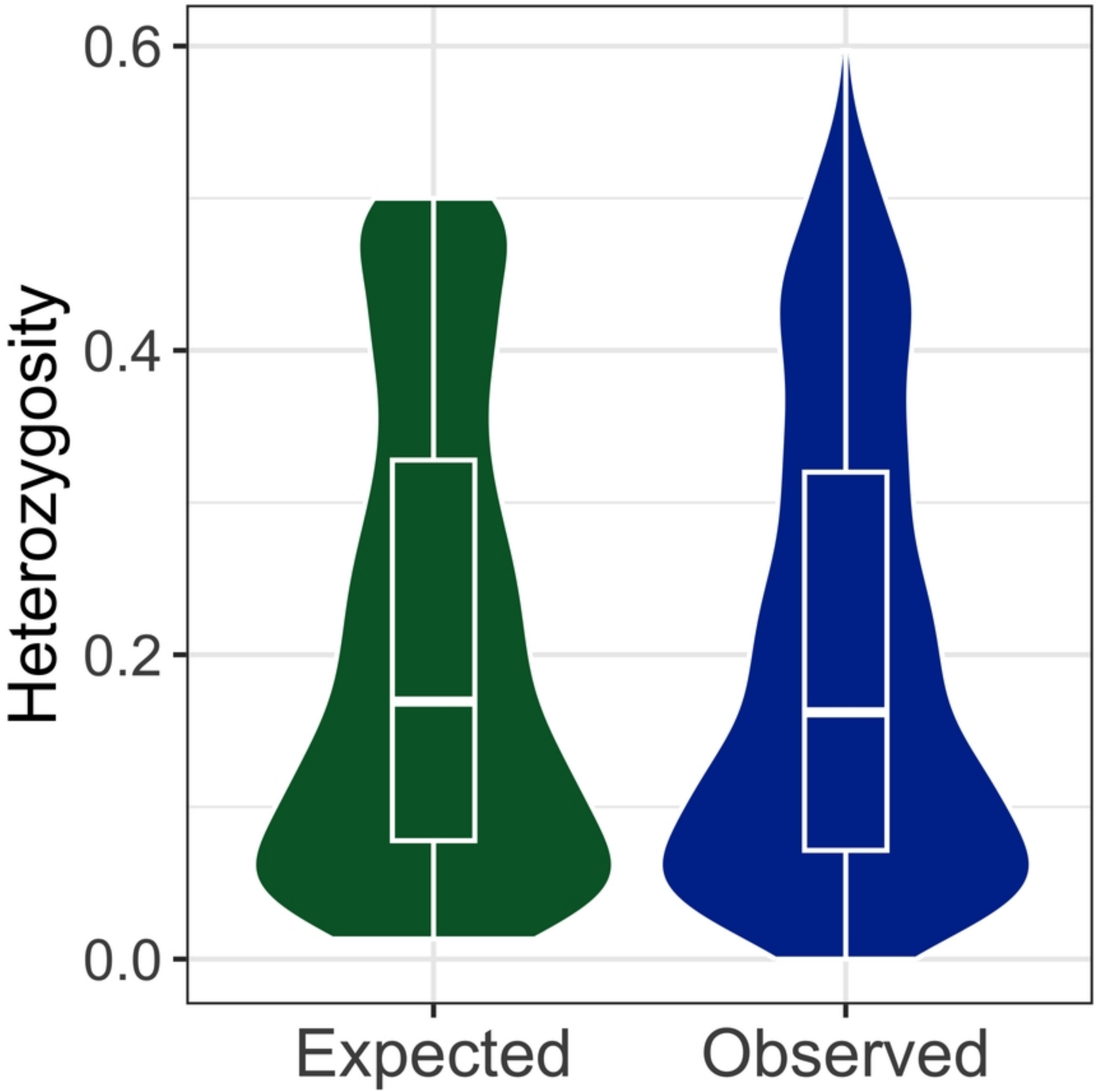

Figure 3

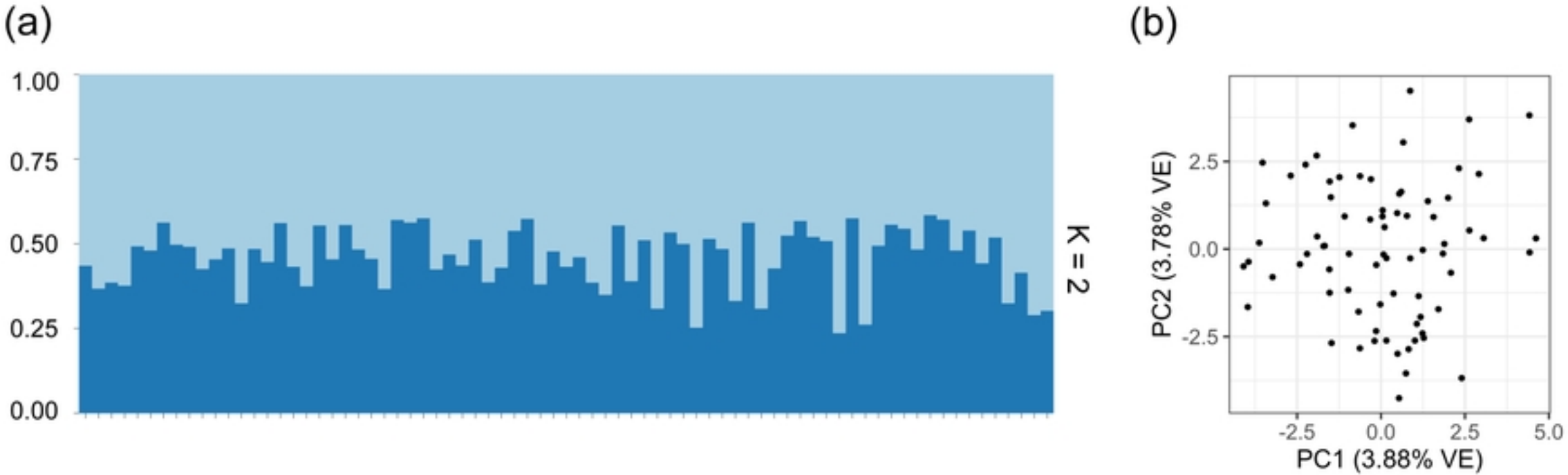

Figure 4

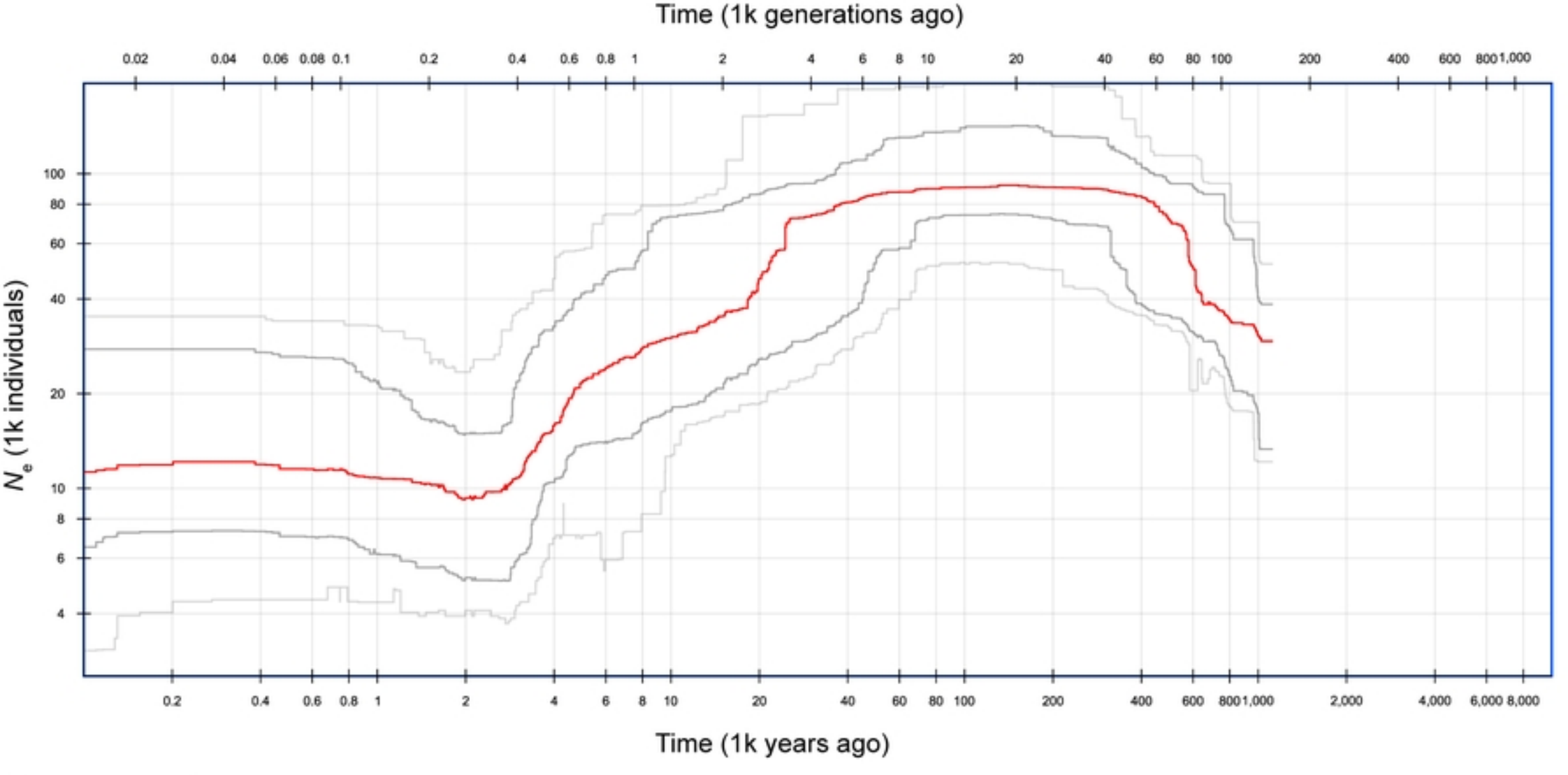
Time (1k generations ago)
0.02
0.04
0.06
0.08
0.1
0.2
0.4
0.6
0.8
1
2
4
6
8
10
20
40
60
80
100
200
400
600
800
1,000
N_e (1k individuals)
100
80
60
40
20
10
8
6
4
0.2
0.4
0.6
0.8
1
2
4
6
8
10
20
40
60
80
100
200
400
600
800
1,000
2,000
4,000
6,000
8,000
Time (1k years ago)

Figure 5